Boson Peak and Fracton of Polymethyl Methacrylate Detected by Terahertz Time-Domain and Low-Frequency Raman Spectroscopies

Shin Nakagawa[1], Tatsuya Mori[1], Yasuhiro Fujii[2], Suguru Kitani[3], Akitoshi Koreeda[2], Hitoshi Kawaji[3], Jae-Hyeon Ko[4], and Seiji Kojima[1]

[1]Division of Materials Science, University of Tsukuba, 1-1-1 Tennodai, Tsukuba, Ibaraki 305-8573, Japan

[2]Department of Physical Sciences, Ritsumeikan University, 1-1-1 Noji-higashi, Kusatsu, Shiga 525-8577, Japan

[3]Laboratory for Materials and Structures, Tokyo Institute of Technology, 4259 Nagatsuta-cho, Midori-ku, Yokohama, Kanagawa 226-8503, Japan

[4]Department of Physics, Hallym University, 1 Hallymdaehakgil, Chuncheon, Gangwondo 24252, Korea

***Abstract*—Terahertz time-domain spectroscopy and low-frequency Raman scattering were performed on polymethyl methacrylate to detect boson peak (BPs) and fractons, which are universal excitations of glass-forming materials. In the infrared spectrum, a BP is observed in the $\alpha(\nu)/\nu^2$ vs. ν plot, where $\alpha(\nu)$ is the absorption coefficient. The log–log plot of $\alpha(\nu)$, $\nu\chi''(\nu)$ and the vibrational density of states exhibit a linear frequency dependence above the BP frequency, where $\chi''(\nu)$ is the imaginary part of the Raman susceptibility. We determined both the infrared light vibration and Raman coupling constants to investigate the appearance of the fractal and fracton dimensions.**

I. INTRODUCTION

DISORDERED materials exhibit universal dynamics in the terahertz (THz) region, which is the so-called boson peak (BP). This is recognized as one of the unsolved problems in glass physics [1]. The BP appears universally in the THz region in the spectrum of the density of states $g(\nu)$ divided by the squared frequency. The spectrum deviates from the Debye model for crystalline systems and has been investigated both experimentally and theoretically for several decades [1,2]. BP in the infrared (IR) spectrum appears in the representation of $\alpha(\nu)/\nu^2$ [3-8], where $\alpha(\nu)$ is the absorption coefficient, although this fact was well-known to past researchers.

Contrarily, a self-similar disordered structure, such as polymer glass and proteins, is expected to exhibit the fractal dynamics, the so-called fracton, which is expected to appear above the BP frequency [9], because the dynamics relate the inter-molecular vibrations of the monomer structure of the self-similarity materials. Thus far, fracton dynamics have been experimentally discussed using low-frequency Raman scattering and inelastic neutron scattering [10,11]. However, few studies have been conducted on fractons using far-IR spectroscopy because the theoretical understanding of the coupling between terahertz light and fracton modes remains inadequate. Recently, Mori *et al*. proposed an expression for the IR light vibration coupling constant $C_{IR}(\nu)$ for the interaction between a BP and fracton [8]; thus, fractons can be detected using THz light.

In this study, we performed terahertz time-domain spectroscopy (THz-TDS) and low-frequency Raman scattering spectroscopy on polymethyl methacrylate (PMMA) to investigate the BP behavior and fracton dynamics. THz-TDS is a spectroscopic technique that uses a femtosecond laser for the emission and detection of a terahertz pulse wave to determine the optical constants of a sample. In our experiment, the THz-TDS measurements of the samples were performed in the frequency range of 0.2–4.5 THz, using a terahertz spectrometer (RT-10000 Tochigi Nikon Co.) [3-8,12-14]. For the light source,

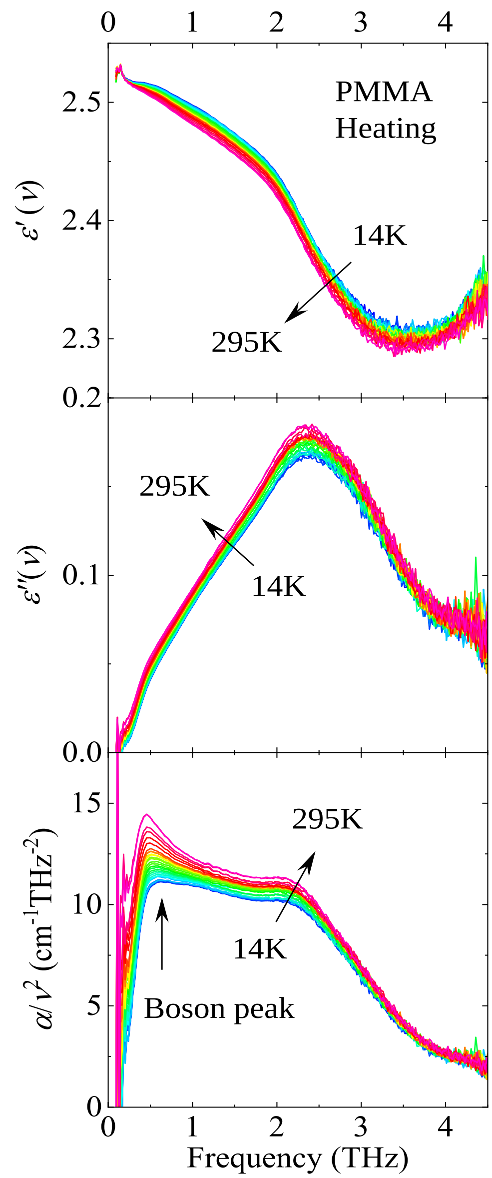

Fig. 1. Temperature dependence of the (a) real and (b) imaginary parts of the complex dielectric constants and (c) the BP curve $\alpha(\nu)/\nu^2$ of PMMA, obtained during the heating process

a mode-locked titanium sapphire laser (Ti: Sapphire laser) was used with a central wavelength of 780 nm, a time width of approximately 100 fs, and a repetition frequency of 80 MHz.

To eliminate the influence of water vapor present in the air, parts of the off-axis ellipsoidal mirrors and sample stage were enclosed in a metal chamber with continuously flowing dry air.

Furthermore, confocal micro-Raman measurements were performed with a depolarized backscattering geometry [15]. A single-frequency solid laser (Oxxius LCX-532S-300) was employed as the excitation source. An inhouse-built microscope with ultra-narrowband notch filters (OptiGrate) was used to focus the excitation laser and detect the Raman-scattered light. The scattered light was analyzed using a single monochromator (Jovin-Yvon, HR320, 1200 grooves/mm) equipped with a charge-coupled device (CCD) camera (Andor, DU420).

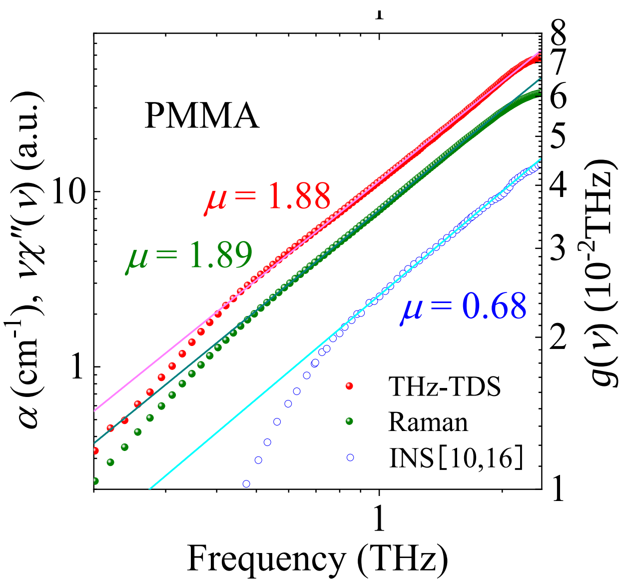

Fig. 2. Comparison of the log–log plots of $\alpha(\nu)$ (red), $\nu\chi''(\nu)$ (green) and $g(\nu)$ [10,16] (blue) of PMMA with frequency. The data of $g(\nu)$ is quoted from previous studies based on inelastic neutron scattering (INS) [10,16].

II. Results

Fig. 1(a)‑1(c) show the temperature dependence of the real ($\varepsilon'(\nu)$) and imaginary ($\varepsilon''(\nu)$) parts of the complex dielectric constant $\varepsilon(\nu)$, and the $\alpha(\nu)/\nu^2$ curve of PMMA during the heating process as obtained via THz-TDS, respectively. As the temperature increases, the value of $\varepsilon'(\nu)$ decreases, whereas that of $\varepsilon''(\nu)$ increases. A shoulder-like structure is observed in the vicinity of 0.4 THz in $\varepsilon'(\nu)$, which indicates that the spectrum below 0.4 THz behaves in resonance rather than in the of the Debye-type dielectric relaxation mode. This type of resonant behavior near the BP frequency has been observed in other glass-forming materials as well and is a behavior observed universally in the variation of $\varepsilon'(\nu)$ [3].

At low temperatures, the BP is observed at approximately 0.5 THz in the $\alpha(\nu)/\nu^2$ curve as a shoulder-like structure, which is due to the $C_{IR}(\nu)$ being governed by proportional terms near the BP frequency. The BP frequency gradually seems to shift to the lower-frequency side as the temperature rises, and its temperature-dependent change corresponds to the relaxation behavior.

Fig. 2 shows the log–log plots of $\alpha(\nu)$ and $\nu\chi''(\nu)$ of PMMA at 295 K. For comparison, the results of the $g(\nu)$ [10,16] of PMMA at 300 K are shown as well. It can be seen that in $\alpha(\nu)$, $\nu\chi''(\nu)$, and $g(\nu)$, the exponential behavior changes in the region above each BP frequency. Above each BP frequency, linear regions are observed in $\alpha(\nu)$, $\nu\chi''(\nu)$, and $g(\nu)$, which are the fracton regions. The slopes of $\alpha(\nu)$ and $\nu\chi''(\nu)$ in the linear region are 1.88 and 1.89, respectively, and the slope of $g(\nu)$ is 0.68. In the fracton region, $g(\nu)$ is proportional to ν^{df-1} (d_f is the fracton dimension); therefore, the fracton dimension d_f is 1.68.

III. Summary

We successfully detected the BP of PMMA using THz-TDS and low-frequency Raman scattering. The BP of PMMA was observed at approximately 0.5 THz. Above the BP frequency, the fracton region appeared in both the IR and Raman spectra. In a poster, we will demonstrate the method to detect fractal dynamics via THz spectroscopy using the formulation of the $C_{IR}(\nu)$ and Raman coupling constant $C_{Raman}(\nu)$. Additionally, we will describe the appearance of the fracton dimension d_f and fractal dimension D_f in $C_{IR}(\nu)$ and $C_{Raman}(\nu)$ above the BP frequency.

References

[1]. T. Nakayama, Rep. Prog. Phys. **65**, 1195 (2002).
[2]. H. Mizuno, H. Shiba, A. Ikeda, Proc. Natl. Acad. Sci. USA **114**, E9767 (2017).
[3]. M. Kabeya, T. Mori, Y. Fujii, A. Koreeda, B.W. Lee, J.H. Ko, S. Kojima, Phys. Rev. B **94**, 224204 (2016).
[4]. W. Terao, T. Mori, Y. Fujii, A. Koreeda, M. Kabeya, S. Kojima, Spectrochim. Acta A **192**, 446 (2018).
[5]. T. Shibata, T. Mori, S. Kojima, Spectrochim. Acta A **150**, 207 (2015).
[6]. J. Zhong, T. Mori, T. Kashiwagi, M. Yamashiro, S. Kusunose, H. Mimani, M. Tsujimoto, T. Tanaka, H. Kawashima, S. Nakagawa, J. Ito, M. Kijima, M. Iji, M. M. Watanabe, K. Kadowaki, Spectrochim. Acta A **244**, 118828 (2021).
[7]. J. Zhong, T. Mori, Y. Fujii, T. Kashiwagi, W. Terao, M. Yamashiro, H. Minami, M. Tsujimoto, T. Tanaka, H. Kawashima, J. Ito, M. Kijima, M. Iji, M. M. Watanabee, K. Kadowaki, Carbohydrate Polymers **232,** 115789 (2020).
[8]. T. Mori, Y. Jiang, Y. Fujii, S. Kitani, H. Mizuno, A. Koreeda, L. Motoji, H. Tokoro, K. Shiraki, Y. Yamamoto, and S. Kojima, Phys. Rev. E **102**, 022502 (2020).
[9]. S. Alexander, R. Orbach, J. Phys. (Paris) **43**, L625 (1982).
[10]. A. Mermet, N. V. Surovtsev, E. Duval, J. F. Jal, J. Dupuy-Philon and A. J. Dianoux, Europhys. Lett. **36**, 279 (1996).
[11]. S. Saikan, T. Kishida, Y. Kanematsu, H. Aota, A. Harada, M. Kamachi, Chem. Phys. Lett. **166**, 358 (1990).
[12]. T. Mori, H. Igawa, and S. Kojima, IOP Conf. Ser.: Mater. Sci. Eng. **54**, 012006 (2014).
[13]. H. Igawa, T. Mori, and S. Kojima, Jpn. J. Appl. Phys. **53**, 05FE01 (2014).
[14]. M. A. Helal, T. Mori, S. Kojima, Appl. Phys. Lett. **106**, 182904 (2015).
[15]. Y. Fujii, D. Katayama, and A. Koreeda, Jpn. J. Appl. Phys. **55**, 10TC03 (2016).
[16]. E. Duval, L. Saviot, A. Mermet, L. David, S. Etienne, V. Bershtein, and A.J. Dianoux, J. Non-Cryst. Solids **307**, 105 (2002).